Understanding hydrological dynamics in Andean basins: An isotope-based study in arid North-Central Chile

Ricardo Oyarzún[1,2,3], Denisse Duhalde[1], José Luis Arumí[4,2], Jan Boll[5], Shelley MacDonell[6,3]

[1]Departamento Ingeniería de Minas, Facultad de Ingeniería, Universidad de La Serena. Benavente 980, La Serena, Chile

[2]Centro de Recursos Hídricos para la Agricultura y la Minería (CRHIAM). Victoria 1295, Barrio Universitario, Concepción, Chile

[3]Centro de Estudios Avanzados en Zonas Áridas (CEAZA). Avenida Raúl Bitrán 1305, La Serena, Chile

[4]Departamento de Recursos Hídricos, Facultad de Ingeniería Agrícola, Universidad de Concepción. Av. Vicente Méndez 595, Chillán, Chile

[5]Civil and Environmental Engineering Department, Voiland College of Engineering and Architecture, Washington State University. Pullman, WA, 99164-2250, USA

[6]Waterways Centre, University of Canterbury. Private Bag 4800, Christchurch, New Zealand

Corresponding Author: Ricardo Oyarzún (royarzun@userena.cl)

Abstract

Mountain ranges cover approximately 24% of the Earth's land mass. These environments have a special relevance in terms of global water supply. However, historically mountain groundwater processes have been generally overlooked or poorly understood, especially in the Andes cordillera. With this in mind, this work aimed to study hydrological processes in four Andean, semi-arid headwater river basins. Along with monthly stable isotope data collection, we carried out a synoptic surface water sampling program in each river on four specific dates for ^{3}H analysis. The latter indicated water of similar age in the rivers of three sub-basins (Derecho, Cochiguaz, Incaguaz), but much older in the fourth (Toro). We assessed different possible explanations for these differences such as effects of past mining activities (El Indio mine), physiographic factors, and snow accumulation and glacier related factors, but none of these were satisfactory. Instead, our findings

point to the activation of faults in response to seismic activity, which induces pumping of fluids (water) from deeper zones, facilitating exfiltration processes in the Toro River sub-basin. This explains the presence of surface waters older than those associated with current meteoric processes. Such geological process should be assessed and eventually accounted for when studying mountain hydrogeological processes, especially in high fractured areas with direct or indirect evidence of geothermal activity.

Keywords

Semi-arid; Andean range; groundwater exfiltration; tritium; stable isotopes.

1. INTRODUCTION

Mountain ranges cover approximately 24% of the Earth's land mass. Since they tend to receive more precipitation than lowland areas, they have a special relevance in terms of global water availability (Sommers and McKenzie, 2020). Indeed, it is estimated that glaciers and seasonal snow pack existing in these settings represent the source of freshwater for more than one-sixth of the world's population (Carroll et al., 2018; Bartnett et al., 2020; Viviroli et al., 2020). Furthermore, the hydrology of mountain areas is important for maintaining local ecosystems (Nauditt et al., 2017), and it is estimated that mountain regions host ca. 50% of the world's biodiversity hotspots (Immerzeel et al., 2020). Finally, the effects of climate change, in particular the rise in temperatures, will be especially important and even amplified in mountainous areas (Vuille et al., 2015; Mayta and Maldonado, 2022). Consequently, studies that address hydrological aspects in these settings have great relevance.

Historically, the main focus in mountain hydrology research has been on glaciers and snowpack (i.e., cryosphere landscape features) while mountain groundwater processes have been generally overlooked or poorly understood (Sommers and McKenzie, 2020 and references within). One reason is because the hydrogeological component was traditionally assumed to be of little importance due to the steep slopes and usually limited soil development in such environments. However, recent studies have highlighted the importance of groundwater storage and discharge in mountain watersheds, particularly their relevance in modulating streamflow during water-scarce periods (e.g., Jódar et al., 2017; Carroll et al., 2018; Guo et al., 2022). Only a few studies on such issues have been developed in the Andean range (Sommers and McKenzie, 2020; Ruiz Pereira et al., 2023). Chile is no exception to the described situation, where the headwaters of many rivers are often poorly monitored (Nauditt et al., 2017). This has resulted in a lack of studies and knowledge of the functioning of hydrological systems in Chilean semi-arid Andean catchments (Navarro et al., 2023).

In this scientific brief, we set out to characterize hydrological processes of four sub-basins of the Elqui River Basin, a semi-arid Andean catchment in North-Central Chile. Our objectives were to employ an isotope approach to: characterize the age of waters in the rivers; explain the hydrological behavior of the sub-basins using a two-year data set; and explore possible reasons for differences among the four sub-basins. We provide a detailed analysis and discussion of plausible explanations and propose a mechanism that explains the observed behavior.

2. AREA OF STUDY

We considered four sub-basins in this study: Derecho, Cochiguaz, Incaguaz, Toro. This study area is in the headwaters of the Elqui River Basin, which includes medium and high mountain zones (Fig. 1).

[Figure 1 here]

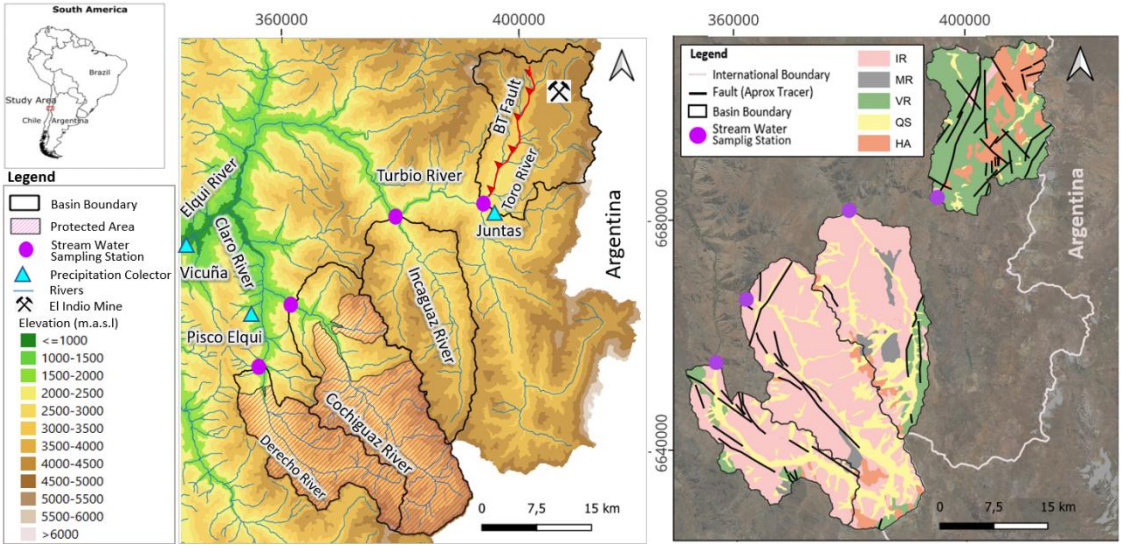

Figure 1. A: Study area with the Derecho, Cochiguaz, Incaguaz and Toro sub-basins; B: Simplified lithology, IR: Igneous rocks; MR: Metamorphic rocks; VR: Volcanic-sedimentary rocks; QS: Quaternary alluvial, glacial, and fluvioglacial sediments; HA: Hydrothermal alteration zones (after Mpodozis and Cornejo (1986), Nasi et al. (1986)).

Climate of the study area is *cold mountain steppe* (Romero et al., 1988), and *cold tundra* at the highest elevations, i.e., above 6,000 masl (Sarricolea et al., 2017), characterized by strong winds, high solar radiation and high precipitation (relative to downstream areas along an E-W transect). Annual precipitation, mainly in the form of snow and concentrated (*ca*. 90%) in the austral winter (Navarro et al., 2023), has a marked orographic dependence, attaining a long-term average of about 300 mm (Favier et al., 2009). Finally, it is important to mention that the area of study, as well as a

large part of the country, has had an extended period of water scarcity (low precipitation) for more than 15 years (Vega-Briones et al. 2023), as shown in Figure 2.

[Figure 2 here]

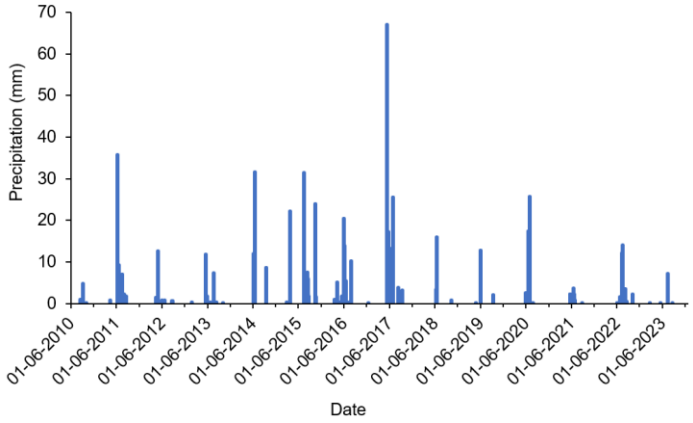

Figure 2. Precipitation amounts measured at the Pisco Elqui weather station, associated with the different events occurring between 2010 and 2023 (CEAZA-MET network, data available at https://www.ceazamet.cl/index.php?pag=mod_estacion&e_cod=8&p_cod=ceazamet).

A brief description of specific characteristics of the four sub-basins is as follows:

Derecho River. Despite some minor agricultural activity in the lower parts, most of this sub-basin (*ca*. 93% of the area, about 315 km^2) was declared a "Nature Sanctuary" in 2015, privately owned by the Comunidad Agrícola Estancia Estero Derecho, with official governmental protection status as Category VI according to the IUCN (i.e., sustainable use of natural resources) (https://www.esteroderecho.cl/). A series of “bofedales” (Andean wetlands) in the upper part of the watershed (along the main course of the river) may have some control on the local water balance (Valois et al., 2021).

Cochiguaz. Along with the Derecho River, but with a greater historical flow, the Cochiguaz River is the main tributary of the Claro River, which has special importance in terms of water quality in the Elqui basin by allowing dilution of metallic contents and reduction of the electrical conductivity of the other main tributary of the upper Elqui, the Turbio River (Oyarzún et al., 2013). As of December 2021, *ca*. 73% of the area of this sub-basin (i.e., ca. 493 km^2) was declared a "Sanctuary of Nature of the Cochiguaz River".

120 *Incaguaz*. Similarly SE-NW oriented as the Derecho and Cochiguaz sub-basins, this area highlights
121 an important geochemical anomaly in river sediments (Cu, Zn, Co, and Y), an indirect indication of
122 a likely low-sulfur mineralization type in the area (Oyarzún et al., 2022).
123 *Toro*. The headwaters of this sub-basin include the El Indio district, a volcanic-rock belt that extends
124 through *ca*. 50 km^2, with intense fracturing and argillic, advanced argillic, and sericitic alteration
125 (Jannas et al., 1999). The El Indio district has several high-sulfidation epithermal deposits (Au-Ag-
126 Cu-As). In particular, the El Indio mine was exploited between 1975 and 2002 attaining worldwide
127 relevance for very high gold grades (over 200 g t^{-1} in the direct export ore) (Oyarzún et al., 2022).
128 It comprised a surface operation (a pit of approximately 15 ha) and multiple levels of underground
129 workings (between 4,050 and 3,820 masl) (Fig. 3). The galleries extended for more than 100 km,
130 from where about 10^6 m^3 of rock were removed. As part of the closure plan of the mine, a tailings
131 dam (Pastos Largos; maximum capacity of 3.3 10^6 m^3, covering an area of about 7 ha) was used as
132 a settling facility to control total concentrations of Cu, Zn, and As in surface waters (Barrick, 2004;
133 Oyarzun et al. 2006; Barrick, 2019).
134
135 [Figure 3 here]

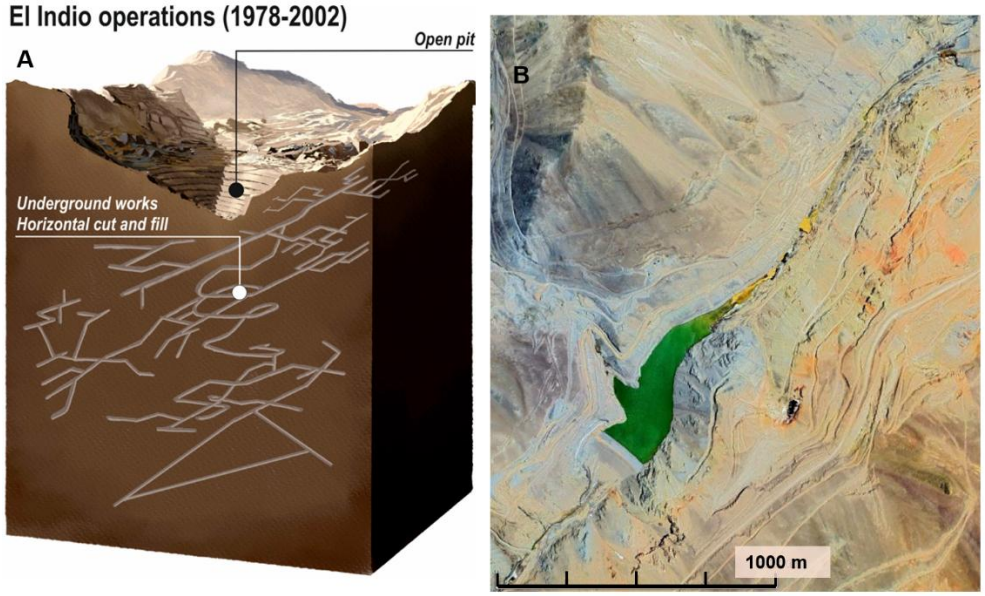

136
137
138 Figure 3. A: Schematic representation of El Indio mine workings (surface and underground); B:
139 Google earth image with the Pastos Largos dam.
140

3. METHODOLOGY

3.1. Water sampling

Data collection included environmental isotope data from precipitation and surface water. We obtained a local meteoric water line (LML) based on precipitation samples from collectors installed at three locations in the basin: Vicuña (630 masl), Pisco Elqui (1,240 masl), and Juntas (2,090 masl), presented in Fig. 1. We collected these samples through the winter of 2022 (n=8) and the winter of 2023 (n=2). To minimize possible evaporation effects, we followed the design proposed by Gröning et al. (2012) for the construction of the collectors. Samples were obtained after each event (not allowing more than two weeks between the precipitation event and sample collection) for ^{2}H and ^{18}O analysis. We collected four additional precipitation samples (1 L) in the months of June and August 2022, that were later analyzed for ^{3}H.

We manually collected stream water samples from August 2021 to August 2023 (monthly frequency) at the outlet of the Derecho, Cochiguaz, Incaguaz, and Toro sub-basins (Fig. 1), in clean 60-mL HDPE bottles with no-headspace lids to avoid evaporation or fractionation. In August and December 2021 and 2022, and January 2024, we took additional samples from each river (same location as ^{18}O and ^{2}H samples) for ^{3}H analysis.

The ^{2}H and ^{18}O analyses were carried out at the Isotope Laboratory at Andrés Bello University (Chile) using Off-axis Integrated Cavity Output Spectroscopy (Maruyama et al., 2013) with a Los Gatos Instrument model TLWIA-45EP, with an accuracy of 0.8‰ for $\delta^{2}H$ and 0.1‰ for $\delta^{18}O$. The ^{3}H analyses were performed at GNS (New Zealand) by electrolytic enrichment and liquid scintillation counting using Quantulus low-level counters (Morgenstern and Taylor, 2009), with a detection limit of approximately 0.025 tritium units (TU). The complete dataset is provided in Supplementary material (SM1).

3.2. Analysis

Regarding stable isotopes, we developed the $\delta^{18}O$ vs. $\delta^{2}H$ diagram and Local Meteoric Water Line (LML). We calculated the deuterium excess (d-excess) of each monthly surface water sample (Eq. 1) as an indicator of evaporation effects on a water sample (Moran et al., 2024).

$$\text{d-excess} = \delta^{2}H - 8\delta^{18}O \quad (1)$$

We calculated the monthly line-conditioned excess (lc-excess) using Eq. 2 as an estimation of the difference between the isotopic signal of each river with respect to its presumed origin (local precipitation) (Landwehr and Coplen, 2006).

$$\text{lc-excess} = \delta^{2}H - a\delta^{18}O - b \quad (2)$$

where a and b are the slope and the intercept of the LML.

With respect to tritium data, we initially considered the approach of Michel et al. (2015). It proposes that under steady-state conditions, the ratio of ^{3}H in precipitation (C_p) to that in surface water (C_s) is of the order of one when runoff rapidly moves through the watershed. This ratio increases ($C_p/C_s > 1$) as water is retained in the watershed on time scales that are relatively long (with respect to the half-life of ^{3}H). In a complementary and more quantitatively approach, we determined the percent of modern water (MW(%)) in the monthly streamflow samples (Eq. 3), following Moran et al. (2024)

$$\text{MW}(\%) = (^{3}H \text{ in sample}/^{3}H \text{ in modern precipitation})*100 \quad (3)$$

3. RESULTS AND DISCUSSION

3.1. Stable isotopes

The dual ^{18}O vs. ^{2}H diagram (Fig. 4) shows an increasing trend with elevation for each sub-basin, i.e., increasing from Derecho to Cochiguaz, then to Incaguaz, and finally to Toro. Figure 4 also includes the LML, i.e., $\delta^{2}H = 8.2\delta^{18}O + 13.1$, which was almost the same as that previously identified by Cuevas (2018) from five precipitation collectors in the upper Elqui (three of them coincidental with our study area). Importantly, some stream samples of Derecho, Cochiguaz, and to a lesser extent of Incaguaz coincide with the LML, whereas this is not the case for stream samples of Toro.

[Figure 4 here]

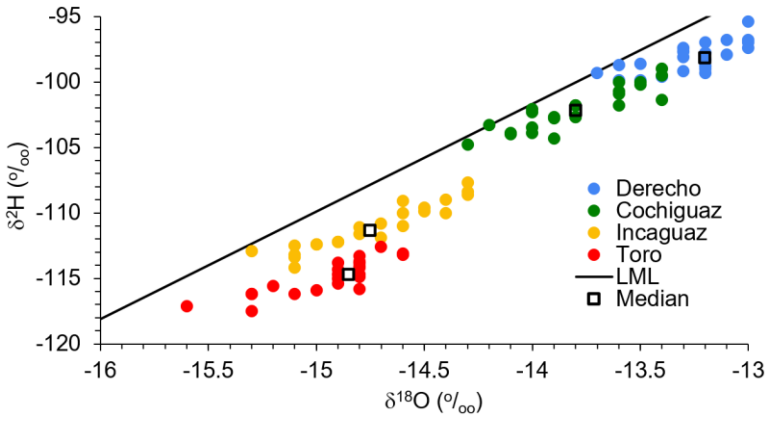

Figure 4. $\delta^{18}O$ vs. $\delta^{2}H$ diagram with the local meteoric water line (LML, $\delta^{2}H = 8.2\delta^{18}O + 13.1$) for surface water samples (closed circles) collected in the Derecho (blue), Cochiguaz (green), Incaguaz (orange) and Toro (red) sub-basins, and median values for each basin (open squares).

We observe that the horizontal displacement ($\delta^{18}O$ axis) of the median isotopic signature values from the LML is clearly greatest for the Toro basin. In the Toro, this horizontal displacement is -5‰, whereas in Incaguaz, Cochiguaz and Derecho the displacement is 2.8, 1.9, and 2.4‰, respectively. A shift in the horizontal axis (i.e., enriched ^{18}O waters) points to the effect of high temperature water-rock interactions (Jasechko, 2019; Daniele et al. 2020; McIntosh and Ferguson, 2021). Thus, such interactions can be inferred in the Toro sub-basin, but not in the other three sub-basins. Also, it is reasonable to expect that the effect of evaporation, which should be of greater importance in the Toro basin because of the Pastos Largos dam, is added to the influence of geothermal water-rock interaction on the horizontal displacement. This is corroborated by the d-excess values for Derecho, Cochiguaz, and Incaguaz that were rather similar to each other, and greater than those observed in the Toro (Fig. 5), which points towards a greater influence of evaporation in the latter. Also, although all values are positive, they are closer to zero in the Toro basin. According to Moran et al. (2024), increasing negative values in d-excess can be associated with evaporation. Likewise, an isotopic exchange with minerals at high temperature conditions translates into negative d-excess values (McIntosh and Ferguson, 2021), a process that would be potentially more important in the Toro sub-basin (i.e., lower d-excess values), consistent with what was presented above.

[Figure 5 here]

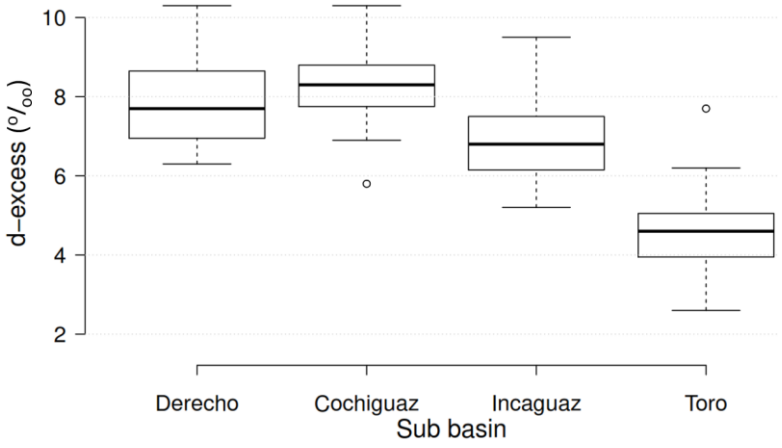

Figure 5. Boxplot of d-excess values for the Derecho, Cochiguaz, Incaguaz and Toro sub-basins.

Differences between Toro and the other three sub-basins is complemented by consideration of lc-excess values (Fig. 6).

[Figure 6 here]

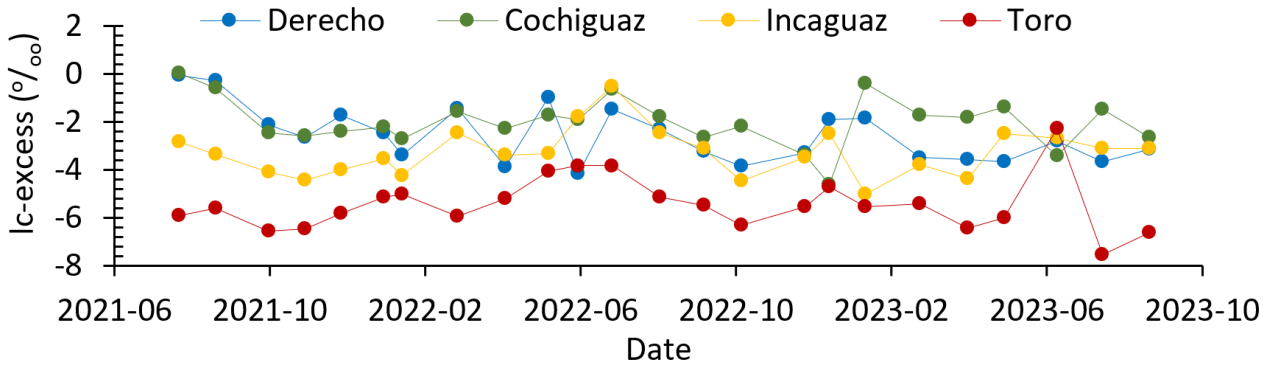

Figure 6. Temporal evolution of lc-excess in surface waters of the four sub-basins.

Since the four sub-basins are located close to each other (the linear distance between the outlets of the Derecho and Toro river basins, the farthest ones, is less than 50 km), it is reasonable

to assume that the waters of the four rivers derive from precipitation events of common origin that fall more or less simultaneously in this mountainous area, in general. Therefore, it would be expected for them to exhibit a rather similar lc-excess. While lc-values tend to be similar for Derecho, Cochiguaz, and to some extent Incaguaz, this was not the case for Toro. Thus, our data support the presence of older waters in the Toro River sub-basin not directly associated with recent precipitation (e.g., that of 2022 and 2023 used in our study).

3.2. Tritium

Values of ^{3}H in precipitation varied from 1.8 to 6.5 (Figure 7) with an average of 4.2. These are consistent with those reported for Andean areas in North-Central Chile. For comparison, Moran et al. (2024) found ^{3}H activities in modern precipitation to be about 3.2+/-0.5 TU in the Chilean Altiplano region. For the Guanaco glacier in the Atacama Region, *ca*. 75 km to the north of our study area, Kinnard et al. (2020) reported values on the order of 4.69+/-0.38 TU for surface snow (i.e., recent precipitation). Ruiz Pereira et al. (2023) indicated values of 4.51 and 8.21 TU for snow samples in the "Monos de Agua" catchment in Central Andes, *ca*. 500 km to the south of upper Elqui.

[Figure 7 here]

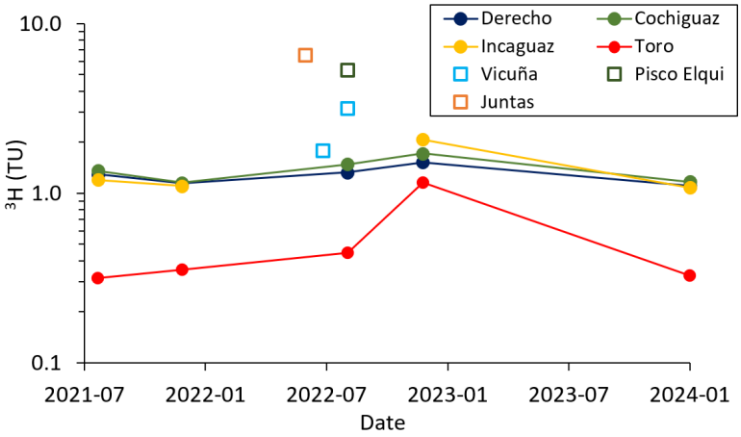

Figure 7. Temporal evolution of ^{3}H in the Derecho, Cochiguaz, Incaguaz and Toro rivers (closed circles) for the sampling campaigns (the Incaguaz sample for August 2022 was lost by the laboratory) and precipitation ^{3}H values (open squares).

Regarding ^{3}H values of the four rivers, two interesting aspects stand out (Fig. 7): (1) in the sampling of December 2022, there was an increase in the ^{3}H levels, especially noticeable in the Toro (which, however, still exhibited lower ^{3}H values than those of the other three rivers). However, this increase is transitory and was not observed in the final sampling of January 2024 when values were like those identified prior to December 2022; (2) the Toro River showed consistently lower values than those of the other three sub-basins, which in turn tend to be generally like each other.

On the first observation, we interpret the generalized increase in the ^{3}H values in the December 2022 sampling by a greater contribution, in general, of surface runoff associated with winter precipitation (especially snowmelt) of that year, which, although low, was the greatest of the last three winters (Fig. 2). Thus, a greater component of young water (i.e., more related to recent precipitation) is present in the runoff of this period.

Regarding the second observation, we can infer that waters of the Derecho, Cochiguaz and Incaguaz rivers have similar ages being younger than those of the Toro River. Based on an approximate average value for C_p on the order of 4.0, it is possible to obtain ratio values (averaged C_p/C_s) on the order of 2.9 to 3.1 for the Derecho, Cochiguaz and Incaguaz rivers, and 9.1 for the Toro River. Therefore, considering the half-life ($t_{1/2}$) of 12.43 years for tritium and under the principle that water with low tritium activity relates to longer transit times than water with high tritium (Stewart and Morgenstern, 2016), a rather important old component exists in surface flow in the sub-basins of the Derecho, Cochiguaz and Incaguaz rivers (i.e., water that is not coming from the precipitation/snowmelt of the same season). However, this situation highly increases in the case of the Toro River. Quantitatively speaking, the percentages of modern water (%MW) were between 30 and 60% in surface streamflow of Derecho, Cochiguaz and Incaguaz, whereas these are significantly lower in the case of Toro (Fig. 8A). We also note that the idea of greater influence of evaporation processes in the case of the Toro sub-basin, when compared to the other three, is reinforced, given the location of the data points on the right of the diagram.

[Figure 8 here]

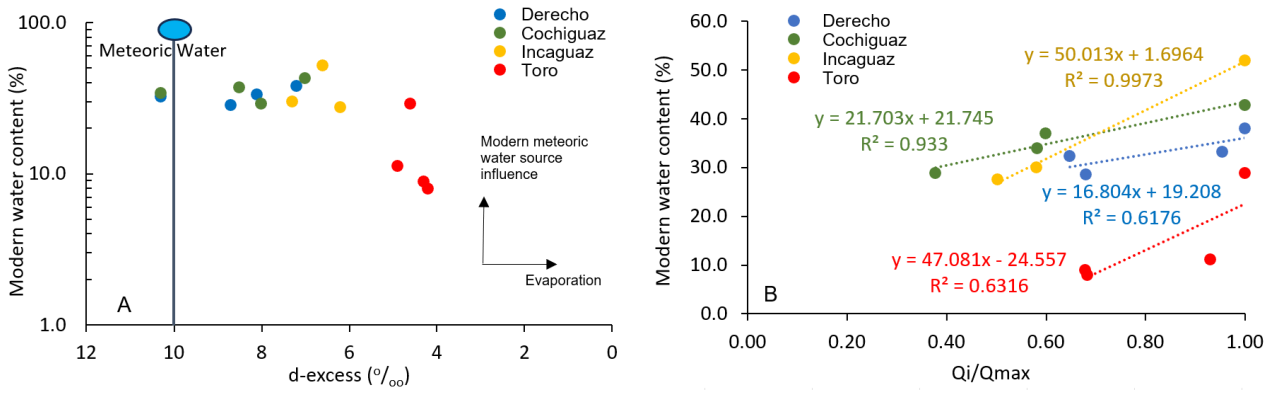

Figure 8. A: Processes controlling water distinctions based on ^{3}H, ^{18}O and ^{2}H (based on a scheme presented in Moran et al., 2024). The inset shows that points further to the right had greater influence of evaporation. B: Ratio of surface discharge (Qi) of August and December 2021 and 2022 to the highest surface discharge of these four campaigns (Q_{max}) for each sub-basin, with respect to the % of modern water recorded (the sampling of January 2024 is not included given the lack of stable isotope data for that date).

Finally, for the four sampling events with simultaneous availability of ^{2}H, ^{3}H, and ^{18}O data (i.e., August and December 2021 and 2022), we observed a higher discharge in 2022 with the maximum flow occurring in December of that year in all cases. This is a direct consequence of the higher precipitation of the winter period of 2022, as already mentioned, which is consistent with the greater percentage of modern water in surface runoff (Fig. 8B). We note an apparent direct relationship between the increase in flow and a greater %MW between the four sampling campaigns considered.

3.3. Possible explanations for the observed hydrological dynamics in the Toro River

Having identified that the Toro River presents an unexpected different hydrological dynamic causing older surface water compared to that of the Derecho, Cochiguaz, and Incaguaz rivers, the question arises as to the reason for this situation. We present and assess four potential explanations as follows.

Possible effect of the El Indio mine works: One explanation might be related to both the underground works of the El Indio mine and the Pastos Largos dam and how they may have affected the

hydrological behavior of the area, explaining the older waters in the Toro River. However, while there seems to be an effect of Pastos Largos on the stable isotopic composition of the Toro River (as already described), it does not explain the differences in water age (which could be related to longer residence times) between sub-basins. Indeed, assuming steady state conditions, we performed a simple calculation of residence time (RT) (Eq. 4)

$$RT = \text{storage volume/flow rate} \quad (4)$$

Considering a storage volume of approximately 4 10^6 m^3 and a flow rate of about 0.35 m^3/s (i.e., average of the Toro River between July 1, 2021 and September 30, 2023), the use of Eq. 4 yields a water residence time of less than a year. This rules out the possibility that the storage volumes associated with the partially inundated gallery system and the Pastos Largos dam explain the observed hydrological behavior.

Physiographic traits: There may be potential hydrologic effects of physiographic factors such as slope and slope exposure of the sub-basins on the amount of precipitation or solar radiation received and, in turn, on snow accumulation and melt, evapotranspiration, infiltration, groundwater recharge and surface water flow (Sommers and McKenzie, 2020). The Toro River sub-basin has a NE-SW orientation that is different from the SE-NW orientation for the other three sub-basins (Fig. 1) and the Toro has somewhat higher altitudes (Table 1). However, no major differences in terms of distributions of elevation, slope, or slope exposure exist. There are also no major differences in terms of surface area, a factor that has been suggested as important for the contribution of groundwater to surface water in high mountains (Sommers and McKenzie, 2020). Physiographic traits, therefore, do not provide a plausible explanation of the different hydrological behavior identified.

[Table 1 here]

348 Table 1. Physiographic characterization and glacier cover in the sub-basins under study (glacier data
349 taken from DGA, 2022).

		Sub-basin			
		Derecho	Cochiguaz	Incaguaz	Toro
Total Area (km^2)		338.2	675.2	477.9	467.2
Elevation min (masl)		1650	1347	1642	2103
Elevation max (masl)		5547	5276	5280	6112
Area (%) by elevation range (masl)	3,000-3,500	17	17	18	15
	3,500-4,000	43	36	33	24
	4,000-4,500	18	21	31	33
Slope (º)	0-22	36	32	30	50
	22-45	59	63	66	49
	45-70	4	4	3	1
	>70	1	1	1	1
Exposure	North	29	24	26	18
	East	27	22	30	25
	South	21	23	18	24
	West	23	31	26	33
	CHE	24.8	24.8	24.6	24.4
N° Glacierets		2	9	1	11
Glacieret area (km^2)		0.035	0.11	0.04	0.18
N° Rock glaciers		43	53	48	6
Rock glaciers area (km^2)		5.35	7.93	4.56	0.51

350 CHE: coefficient of homogeneity of exposure (CHE), calculated as the fourth root of the product of
351 the areas (as a percentage) of each exposure class (Barrera et al., 2020)
352
353 *Snow and glacier accumulation and melt*: Uneven spatial and temporal distributions of glaciers and
354 snow cover could influence surface flows (e.g., Ayala et al., 2023). Regarding snow, a direct analysis
355 of the temporal distribution of accumulated snow for the period 2021-2023 (presented, for
356 comparison purposes, as a percentage of the area of each sub-basin covered by snow), revealed no
357 differences between sub-basins (Fig. 9). In addition, practically the entire snow cover melts during
358 the spring, so we cannot associate the presence of old water in surface streams with snowmelt
359 accumulated at the surface from previous years.
360
361 [Figure 9 here]
362

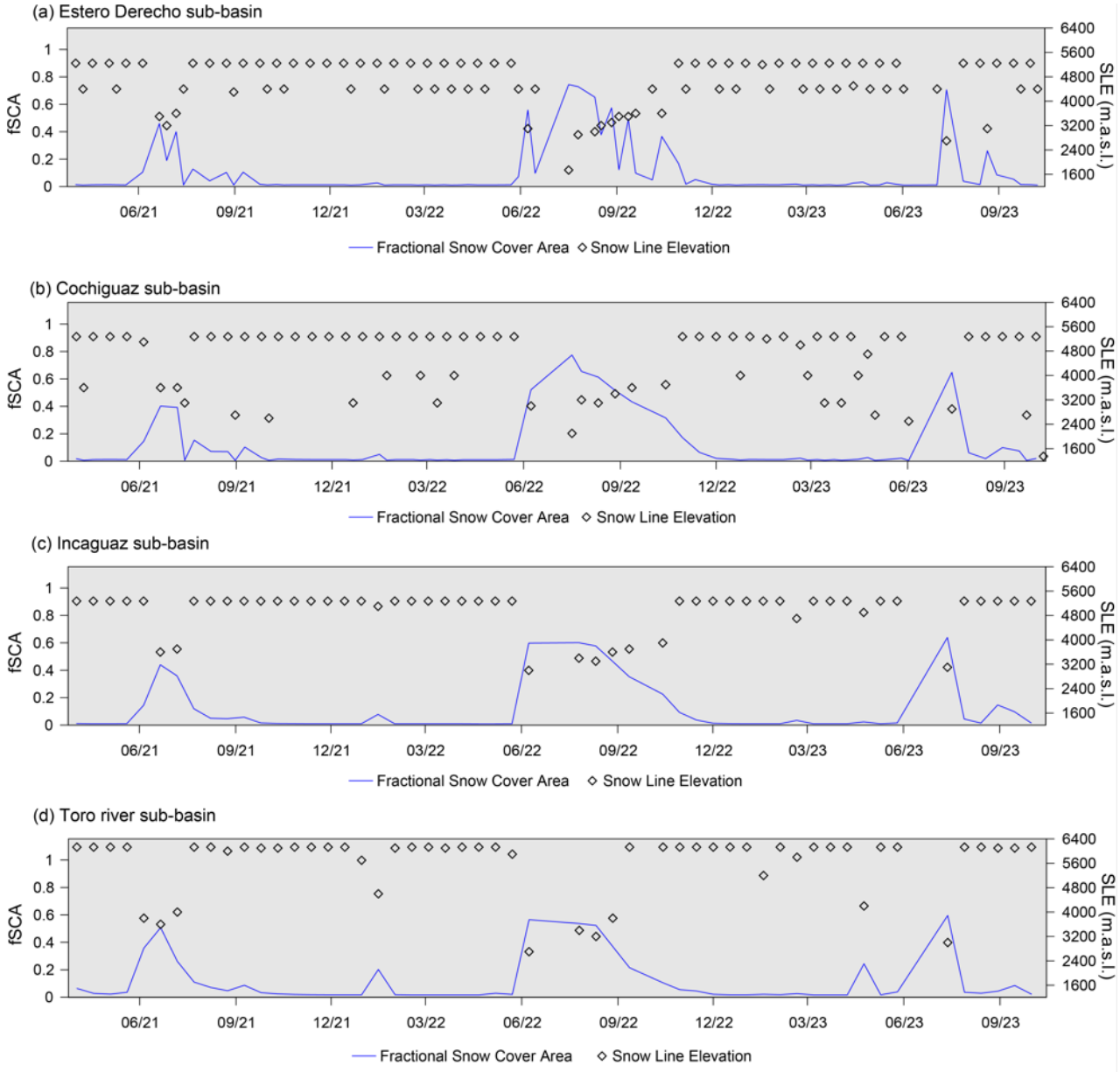

Figure 9. Time evolution of fractional of snow cover area (fSCA) and snow line elevation (SLE) for the Derecho, Cochiguaz, Incaguaz, and Toro sub-basins.

In some areas it is possible to find examples of the effects of uneven distributions of glaciers on the hydrological behavior in rivers downstream (Ohlanders et al., 2013; Sommers and McKenzie, 2020). With respect to debris-free (or white) glaciers, Yáñez et al. (2023) stated that their presence in the Elqui basin as a whole is very limited. Most of the ice volume is in the Tapado Glacier, which is in the La Laguna sub-basin, next to the Toro sub-basin but outside of the current study area. Thus, we consider the effect of white glaciers on the hydrological behavior of the Toro River negligible

compared to the other three sub-basin. While there are also glacierets, i.e., very small glaciers of less than 0.25 km^2 (Cogley et al., 2011), in total they cover a very small area, so they are unlikely to be influential at the catchment scale as well. We also note that it is possible to find rock glaciers in the four sub-basins (Table 1), but the assessment of their hydrological contribution remains very difficult and uncertain (Schaffer et al., 2019). In any case, if we assume that rock glaciers have the capability to store water over decades to centuries (Schaffer et al., 2019), this effect should be of lower importance at the Toro sub-basin, where the area of rock glaciers is the smallest of the four sub-basins. Thus, factors associated with snow accumulation or the presence of glaciers (or glacierets) also do not provide a plausible explanation for the different hydrological dynamic exhibited by the Toro sub-basin.

Geological control: A final analysis relates to geology, an important factor in the comprehension of the hydro(geo)logical dynamics in mountain settings. Whereas in the sub-basins of Derecho, Cochiguaz and Incaguaz rivers the geology is mostly intrusive igneous rocks (*ca*. 62% of the surface area) and areas of fluvio-glacial sedimentary deposits (*ca*. 19-23%), in the Toro sub-basin volcanic and pyroclastic rocks dominate the geology (Mpodozis and Cornejo, 1986; Nasi et al., 1986). The latter are affected by pervasive hydrothermal alteration and intense faulting, in which the Baños del Toro high-angle reverse fault (Deyell et al., 2004) stands out (Fig. 1). The Baños del Toro thermal-spring is related to this fault, and its waters were described by Strauch et al. (2006) as a probable mixture of deep circulating fluids and meteoric waters. Likewise, Benavente et al. (2016) described the relation between meteoric waters and its circulation through deep regional structures associated to the San Ramón-Pocuro fault zone to the presence of thermal springs in central Chile, some 500 km to the south of the study area of the current work.

With this in mind, we postulate that the Toro sub-basin, unlike the other three, exhibits an important process of exfiltration, i.e., groundwater discharging to surface water (Sommers and McKenzie, 2020), favored by a greater presence of lineaments and structural features, especially the high-angle Baños del Toro reverse fault, acting as preferential pathways for ascending groundwater flow. This exfiltration provides a very plausible explanation for the older water observed in the Toro River. This is consistent with the study of Marti et al. (2023), for the Clarillo River basin, an ungauged catchment with an area of 130 km^2 located some 500 km south of our study area (33°50′S). These authors indicated a major increase (*ca*. 50%) in streamflow over just a 1 km distance, which they explain as the consequence of an important contribution to baseflow from groundwater exfiltration, related to a regional N-S fault and secondary E-W local faults that are thought to export

406 groundwater from a neighboring subcatchment up to the resurgence area. Taucare et al. (2020) also
407 described groundwater outflows from NW–SE fractures associated with the Pocuro fault zone in
408 pre-mountain areas (i.e., western Andean front form the principal cordillera) in the Aconcagua basin
409 at 32°50′S.
410 An exfiltration process can be enhanced by strong fracturing as it is the case in the study area
411 (e.g., Oyarzun et al. 2007); faulting processes destroy the integrity of the rock mass allowing an
412 increase in rock permeability (e.g., Tripp and Vearncombe, 2004; Faulkner et al., 2010; Zhang et al.
413 2021). However, as noted by Keegan-Treolar et al. (2022), while springs and faults have been
414 studied separately, their interrelation and effects on hydrogeological processes has received less
415 attention. Indeed, the nature and cause of this type of exfiltration process is not generally addressed
416 in the literature related to hydrogeological/hydrological, high-altitude mountain belts (Sommers and
417 McKenzie, 2020). In addition, minor attention has been paid in the past to the transport mechanism
418 required to move ascending fluids along fault zones (e.g., Sibson et al. 1975). In this regard, the
419 consideration of knowledge from other disciplines (e.g., structural geology, petroleum, mining)
420 could favor the understanding of fault properties and their hydrological relevance (Keegan-Treolar
421 et al. (2022). Some answers regarding the many factors that may be playing a role in the study area
422 can be provided by the pioneering work on faults and fluids developed by R. Sibson between the
423 1970's and 1980's (e.g., Sibson et al., 1975; Sibson, 1987; Sibson et al., 1988) that changed the
424 perception of how deep-seated waters moved upwards along faults in relation to seismic activity.
425 What is proposed in the referred literature relates to the activation of faults in response to seismic
426 activity, which induces the pumping of fluids (here water) from deeper zones to the surface with
427 older ages associated with current meteoric processes (Fig. 10).
428
429 [Figure 10 here]
430
431

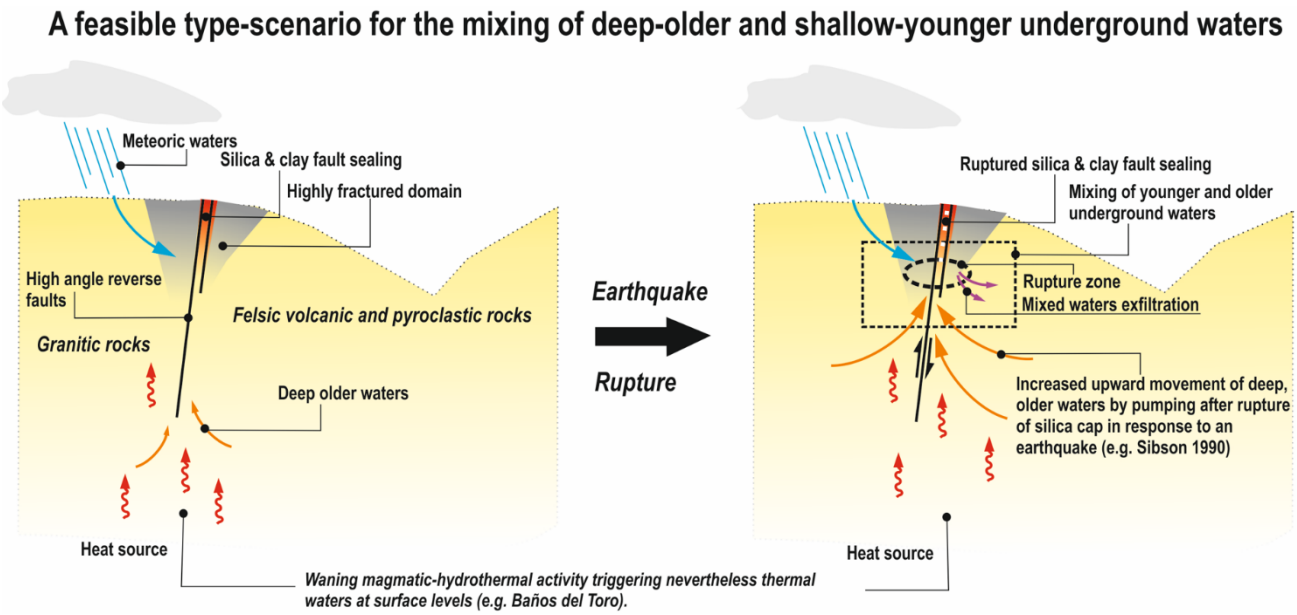

Figure 10. Schematic (not to scale) depicting the main structural and hydrological elements that would account for the ascent of deep, older (and hotter) waters. Partially based on Sibson et al. (1988); Sibson (1990); and Deyell et al. (2004).

In simple terms, the fault is sealed by an impermeable barrier while fluid pressure rises in the lower region until a seismic rupture occurs at the base of the barrier. After the seal has been breached, fluids can rise freely along the fault and there deep, older fluids ascend and eventually mix with younger fluid of more recent meteoric origin. In this regard, high-angle reverse faults, such as that of the Baños del Toro, can act as valves, resulting in cyclic fluctuations of fluid pressure from supralithostatic to hydrostatic values (Sibson et al. 1988). Seismic fault failure results in structural permeability within the rupture zone, allowing the fast ascent of the geo-pressured waters at depth, which in turn is followed by self-sealing of the ruptured fault zone, the re-accumulation of fluid pressure, and eventually the repetition of the cycle (Sibson et al. 1988).

While it has been recognized that earthquakes can have a significant effect on fault-controlled spring systems, the review of Keegan-Treolar et al. (2022) shows that these impacts are rarely considered in many cases. Regarding our work, although it is not possible to directly evaluate the proposed mechanism based on the data collected during the two years of surface water sampling, historical information can be considered as an indirect way to assess the validity of this explanation. This is addressed as follows.

452 It is well-known that the study area, and Chile in general, is subject to permanent seismic
453 activity. In particular, on September 16, 2015, the Coquimbo region experienced a major earthquake
454 of 8.3 degrees on the Richter scale, which had several aftershocks, including a major one of 6.9
455 (degrees on the Richter scale) on November 11, 2015. Oyarzún et al. (2019) described the effect of
456 these earthquake events on the emptying of a rather small aquifer in a fractured rock massif near the
457 Elqui coastal area. Here, considering the same events but focusing in the current study area, it is of
458 particular interest that the Sept 16, 2015 event was followed by a period of approximately two weeks
459 (zone "A" in Fig. 11) of unusually increased discharge in the Toro River (reversing an ongoing
460 downward trend), which was not observed in the Derecho and Cochiguaz rivers. Coinciding with
461 the increase in flow there was a transient increase in water temperature as well.
462
463 [Figure 11 here]
464

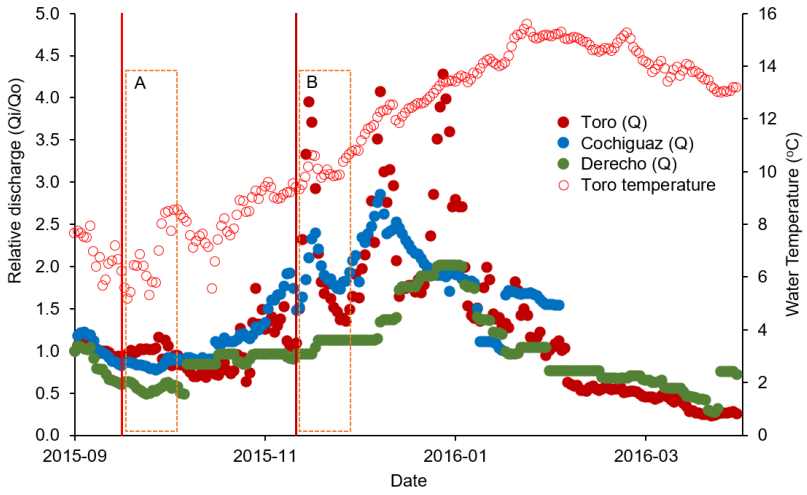

465

466 Figure 11. Variation in relative discharge (Q_i/Q_o, with Q_i being the average discharge of day "i" and
467 Q_o the average discharge of September 1, 2015) of Toro, Derecho and Cochiguaz rivers (closed
468 circles), and water temperature (open circles) of the Toro river (after DGA data taken from
469 https://snia.mop.gob.cl/dgasat/pages/dgasat_param/dgasat_param.jsp?param=1). Vertical red lines
470 show the date of occurrence of the 8.3 and 6.9 (Richter degrees) seismic events; A and B denotes
471 ca. two-weeks periods after those events.

472

473 Following the major aftershock on November 11, 2015, another period of approximately two
474 weeks (zone "B" in Fig. 9) showed the same increase of flow and temperature in the Toro River.

475 Although in this case an increase in surface discharge was also observed in the Derecho and
476 Cohiguaz rivers, that increase was much smaller compared to that observed in the Toro River, and
477 likely was mainly related to the onset of the late-spring/summer snow melting in Derecho and
478 Cochiguaz sub-basins.
479 In summary, it is reasonable in the Toro case, that an exfiltration mechanism allows the
480 ascent of deeper and older groundwater, effectively explaining the situation clearly noticed with the
481 ^{3}H analyses and supported by the ^{2}H, ^{18}O data. In other words, the presence of older waters, and
482 therefore a particular and different hydrological dynamic, with respect to the other sub-basins
483 studied. Our data analyses provide indirect, supporting evidence for the rise of deep waters affected
484 by the waning magmatic activity that still exists in the Toro sub-basin, the latter as inferred from the
485 presence of the Baños del Toro thermal-spring and other thermal-springs elsewhere (Maksaev et al.,
486 1984). There is evidence (indirect but consistent) of the effect of seismic activity on fault behavior
487 and its effects on the differential hydrological dynamic of the Toro River.
488
489
490 **4. CONCLUSIONS**
491 Based on the use of environmental tracers (^{3}H, ^{18}O, ^{2}H), we observed different hydrological behavior
492 in the Toro River sub-basin compared to three nearby ones (Derecho, Cochiguaz, and Incaguaz
493 rivers sub-basins). We evaluated possible explanations for this outcome.
494 Although we initially thought that the facilities of an important mining site, currently in the
495 closure stage (in particular the volume associated with underground works and a tailings dam used
496 as a sedimentation pond), could have played a role in the hydrological behavior observed, a simple
497 residence time calculation ruled out this possibility. We also could not attribute the presence of older
498 waters in Toro to specific different physiographic features in that basin (compared to the other three),
499 or to differences in seasonal distributions of snow and glaciers. Our analysis instead pointed towards
500 the role of geological features of the Toro River sub-basin, integrating concepts associated with the
501 ascent of fluids in fault zones, to obtain a feasible explanation of the observed hydrological dynamic.
502 We postulate that the hydrological behavior in the Toro sub-basin is related to the activation of faults
503 in response to seismic activity. Water from deeper zones is pumped upward causing the presence of
504 water at the surface that is older than those associated with current meteoric processes. We explain
505 the proposed occurrence of this fault-induced water flow process by indirect information associated
506 with a major seismic event that occurred in 2015, as well as the description of a similar situations in

nearby basins in the central zone of Chile. These findings support the notion that geological processes, such as earthquake induced fault activities, should be assessed, and eventually accounted for when studying mountain hydrogeological processes, especially in high fractured areas and with direct or indirect evidence of geothermal activity.

ACKNOWLEDGMENTS

We discussed the structural geology setting and the water pumping model with Roberto Oyarzun, retired Associated Professor of Mining Geology of the Complutense University (Madrid, Spain), who also revised the original manuscript and prepared Figure 10. We also thank Eduardo Yáñez for his help in the snow cover analysis (Figure 9). This work was supported by ANID/FONDECYT/1210177, ANID/FONDAP/15130015, ANID/FONDAP/1523A0001, and the CRP F33026 initiative (IAEA). The paper greatly benefited from the comments of two anonymous reviewers and the associate editor (Dr. McNamara).

REFERENCES

Ayala, A.., Schauwecker, S., and MacDonell, S. 2023. Spatial distribution and controls of snowmelt runoff in a sublimation-dominated environment in the semiarid Andes of Chile. Hydrology and Earth System Sciences 27, 3463–3484. https://doi.org/10.5194/hess-27-3463-2023.

Barrera, C., Núñez, J., Souvignet, M., Oyarzún, J., Oyarzún, R. 2020. Streamflow elasticity, in a context of climate change, in arid Andean watersheds of north-central Chile, Hydrological Sciences Journal 65(10), 1707-1719. DOI: 10.1080/02626667.2020.1770764

Barnett, T., Adam, J., Lettenmaier, D. 2005. Potential impacts of a warming climate on water availability in snow-dominated regions. Nature 438, 303–309. https://doi.org/10.1038/nature04141

Barrick, 2004. Plan cierre laguna de sedimentación y tranque de relaves Pastos Largos. Available at https://snia.mop.gob.cl/repositoriodga/handle/20.500.13000/7328. Accessed November 2023

Barrick. 2019. Plan de Cierre de El Indio, Efecto Cierre Tranque Pastos Largos: Análisis resultados modelo y prueba de terreno. Expediente de la Norma Secundaria de Calidad Ambiental para la protección de las aguas continentales superficiales de la cuenca del río Elqui. Available at https://planesynormas.mma.gob.cl/normas/expediente/index.php?tipo=busqueda&id_expediente=930202. Accessed October 2023

Benavente, O., Tassi, F., Reich, M., Aguilera, F., Capecchiacci, F., Gutiérrez, F., Vaselli, O., Rizzo, A. 2016. Chemical and isotopic features of cold and thermal fluids discharged in the Southern Volcanic Zone between 32.5°S and 36°S: Insights into the physical and chemical processes controlling fluid geochemistry in geothermal systems of Central Chile. Chemical Geology
420, 97-113.

Carroll, R.W.H., Bearup, L.A., Brown, W., Dong, W., Bill, M., Willlams, K.H. 2018. Factors controlling seasonal groundwater and solute flux from snow-dominated basins. Hydrological Processes 32, 2187-2202

Cepeda, J., Cabezas, R., Robles, M., Zavala, H. 2008. Antecedentes generales de la cuenca del río Elqui (Región de Coquimbo, Chile). In: J. Cepeda, ed. Los sistemas naturales de la cuenca del río Elqui (región de Coquimbo, Chile): Vulnerabilidad y cambio del clima. La Serena, Chile: Ediciones Universidad de La Serena, 13–37. Available at https://www.parc.ca/mcri/pdfs/books/cepeda/1.pdf. Accessed October 2019.

Cogley, J.G., Hock, R., Rasmussen, L.A., Arendt, A.A., Bauder, A., Braithwaite, R.J., Jansson, P., Kaser, G., Möller, M., Nicholson, L., Zemp, M. 2011, Glossary of Glacier Mass Balance and Related Terms, IHP-VII Technical Documents in Hydrology No. 86, IACS Contribution No. 2, UNESCO-IHP, Paris. Available at https://unesdoc.unesco.org/ark:/48223/pf0000192525

Cuevas, J. 2018. Caracterización isotópica de la parte alta de la Cuenca del río Elqui. Memoria de Título, Ingeniería Civil Ambiental, Universidad de La Serena, 40 p.

Daniele, L., Taucare, M., Viguier, B., Arancibia, G., Aravena, D., Roquer, T., Sepúlveda, J., Molina, E., Delgado, A., Muñoz, M., Morata, D. 2020. Exploring the shallow geothermal resources in the Chilean Southern Volcanic Zone: Insight from the Liquiñe thermal springs. Journal of Geochemical Exploration 218. https://doi.org/10.1016/j.gexplo.2020.106611.

572 Deyell, C.L., Bissig, T., Rye, R.O. 2004. Isotopic Evidence for Magmatic-Dominated Epithermal Processes
573 in the El Indio-Pascua Au-Cu-Ag Belt and Relationship to Geomorphologic Setting. Society of Economic
574 Geologists, Special Publication 11, 55-73
575
576 DGA. 2022. Inventario Público de Glaciares. Dirección General de Aguas, Ministerio de Obras Públicas,
577 Gobierno de Chile. Available at https://dga.mop.gob.cl/Paginas/InventarioGlaciares.aspx. Accessed
578 November 2023
579
580 Favier, V., Falvey, M., Rabatel, A., Praderio, E., López, D. 2009. Interpreting discrepancies between
581 discharge and precipitation in high-altitude area of Chile's Norte Chico region (26–32ºS). Water Resources
582 Research 45:W02424. doi:https://doi.org/10.1029/2008WR006802
583
584 Faulkner, D.R., Jackson, C.A.L., Lunn, R.J., Schlische, R.W., Shipton, Z.K., Wibberley, C.A.J., Withjack,
585 M.O. 2010. A review of recent developments concerning the structure, mechanics and fluid flow properties
586 of fault zones. Journal of Structural Geology, 32 (11), 1557-1575. https://doi.org/10.1016/j.jsg.2010.06.009.
587
588 Gröning, M., Lutz, H.O., Roller-Lutz, Z., Kralik, M., Gourcy, L., Pöltenstein, L. 2012. A simple rain collector
589 preventing water re-evaporation dedicated for δ18O and δ2H analysis of cumulative precipitation samples.
590 Journal of Hydrology 448-449, 195-200.
591
592 Guo, X., Feng, Q., Yin, Z., Si, J., Xi, H., Zhao, Y. 2022. Critical role of groundwater discharge in sustaining
593 streamflow in a glaciated alpine watershed, northeastern Tibetan Plateau. Science of The Total Environment
594 822. https://doi.org/10.1016/j.scitotenv.2022.153578.
595
596 Immerzeel, W.W., Lutz, A.F., Andrade, M., Bahl, A., Biemans, H., Bolch, T., Hyde, S., Brumby, S., Davies,
597 B.J., Elmore, A.C., Emmer, A., Feng, M., Fernández, A., Haritashya, U., Kargel, J.S., Koppes, M.,
598 Kraaijenbrink, P.D.A., Kulkarni, A.V., Mayewski, P.A., Nepal, S., Pacheco, P., Painter, T.H., Pellicciotti, F.,
599 Rajaram, H., Rupper, S., Sinisalo, A., Shrestha, A.B., Viviroli, D., Wada, Y., Xiao, C., Yao, T., Baillie, J.E.
600 2020. Importance and vulnerability of the world's water towers. Nature 577, 364-369.
601 https://doi.org/10.1038/s41586-019-1822-y
602
603 Jannas, R.R., Bowers, T.S., Petersen, Ul., Beane, R.E. 1999. High-Sulfidation Deposit Types in the El Indio
604 District, Chile. Special publications of the Society of Economic Geologists. Geology and Ore Deposits of the
605 Central Andes. DOI https://doi.org/10.5382/SP.07.07

606
607 Jasechko, S. 2019. Global isotope hydrogeology—review. Reviews of Geophysics, 57
608 https://doi.org/10.1029/2018RG000627
609
610 Jódar, J., Cabrera, J.A., Martos-Rosillo, S., Ruiz-Constán, A., González-Ramón, A., Lambán, L.J., Herrera,
611 C., Custodio, E. 2017. Groundwater discharge in high-mountain watersheds: A valuable resource for
612 downstream semi-arid zones. The case of the Bérchules River in Sierra Nevada (Southern Spain). Science of
613 the Total Environment 593–594, 760-772. https://doi.org/10.1016/j.scitotenv.2017.03.190.
614
615 Kinnard, C., Ginot, P., Surazakov, A., MacDonell, S., Nicholson, L., Patris, N., Rabatel, A., Rivera, A.,
616 Squeo, F. 2020. Mass balance and climate history of a high altitude glacier, desert Andes of Chile. Frontiers
617 in Earth Science, 8: 40. DOI 10.3389/feart.2020.00040
618
619 Landwehr, J., & Coplen, T. (2006). Line-conditioned excess: A new method for characterizing stable
620 hydrogen and oxygen isotope ratios in hydrologic systems. Isotopes in Environmental Studies (pp. 132–135).
621 Monaco: International Atomic Energy Agency.
622
623 Maksaev, V., Moscoso, R., Mpodozis, C., Nasi, C. 1984. Las unidades volcánicas y plutónicas del Cenozoico
624 superior en la alta Cordillera del Norte Chico (29º-31º S): Geología, alteración hidrotermal y mineralización.
625 Revista Geológica de Chile 21, 11-51
626
627 Marti, E., Leray, S., Villela, D., Maringue, J., Yáñez, G, Salazar, E., Poblete, F., Jimenez, J., Reyes, G.,
628 Poblete, G., Huamán, Z., Figueroa, R., Araya, J., Sanhueza, J., Muñoz, M., Charrier, R., Fernández, G. 2023.
629 Unravelling geological controls on groundwater flow and surface water-groundwater interaction in mountain
630 systems: A multi-disciplinary approach. Journal of Hydrology 623, 129786
631
632 Maruyama, S., Tanaka, Y., Hirayama, S., Kusakabe, M., Zhang, J., Nakano, T. 2013. High-precision
633 measurements of water isotopes using laser absorption spectroscopy. Geochemical Journal 47(6), 675-682.
634 https://doi.org/10.2343/geochemj.2.0233
635
636 Mayta, C., Maldonado, A. 2022. Climatic and ecological changes in the subtropical high Andes during the
637 last 4,500 years. Frontiers in Earth Sciences 10: 833219. DOI 10.3389/feart.2022.833219
638

McIntosh, J.C., Ferguson, G. 2021. Deep meteoric water circulation in Earth's Crust. Geophysical Research Letters 48, e2020GL090461. https://doi.org/10.1029/2020GL090461

Michel, R.L., Aggarwal, P-. Araguas-Araguas, L., Kurttas, T., Newman, B.D., Vitvar, T. 2015. A simplified approach to analyzing historical and recent tritium data in surface waters. Hydrological Processes 29, 572-578.

Moran, B.J., Boutt, D.F., Munk, L.A., Fisher, J.D. 2024. Contemporary and relic waters strongly decoupled in arid alpine environments. PLOS Water 3(4): e0000191. https://doi.org/10.1371/journal.pwat.0000191

Morgenstern, U., Taylor, C.B. 2009 Ultra low-level tritium measurement using electrolytic enrichment and LSC. Isotopes in Environmental and Health Studies 45(2), 96-117

Mpodozis, C., Cornejo, P. 1986. Hoja Pisco Elqui. Carta Geológica de Chile, 1:250.000. Servicio Nacional de Geología y Minería, Gobierno de Chile

Nasi, C., Mosoco, R., Maksaev, V. 1986. Hoja Guanta. Carta Geológica de Chile, 1:250.000. Servicio Nacional de Geología y Minería, Gobierno de Chile

Nauditt, A., Soulsby, C., Birkel, C., Rusman, A., Schüth, C., Ribbe, L., Álvarez, P., Kretschmer, N. 2017. Using synoptic tracer surveys to assess runoff sources in an Andean headwater catchment in central Chile. Environmental Monitoring and Assessment 189, 440. https://doi.org/10.1007/s10661-017-6149-2

Navarro, G., MacDonell, S., Valois, R. 2023. A conceptual hydrological model of semiarid Andean headwater systems in Chile. Progress in Physical Geography 47(5). DOI 10.1177/03091333221147649

Ohlanders, N., Rodriguez, M., McPhee, J. 2013. Stable water isotope variation in a Central Andean watershed dominated by glacier and snowmelt. Hydrology and Earth System Science 17, 1035–1050.

Oyarzún J., Carvajal, M.J., Maturana, H., Núñez, J., Kretschmer, N., Amézaga, J., Rötting, T., Strauch, G., Thyne, G., Oyarzún, R. 2013. Hydrochemical and Isotopical Patterns in a Calc-Alkaline Cu- and Au-Rich Arid Andean Basin: The Elqui River Watershed, North Central Chile. Applied Geochemistry, 33: 50-63.

672 Oyarzún, J., Núñez, J., Fairley, J.P., Tapia, S., Alvarez, D., Maturana, H., Arumí, J.L., Aguirre, E., Carvajal,
673 A., Oyarzún, R. 2019. Groundwater Recharge Assessment in an Arid, Coastal, Middle Mountain Copper
674 Mining District, Coquimbo Region, North-central Chile. Mine Water and the Environment 38(2), 226-242.
675 https://doi.org/10.1007/s10230-019-00603-7
676
677 Oyarzún, J., Maturana, H., Paulo, A., Lillo, J., Pastén, P., Núñez, J., Duhalde, D., González, C., Portilla, A.,
678 Oyarzún, R. 2022. Environmental Aspects of a Major ARD Source at El Indio Au-Cu-As District, North-
679 Central Chile. Mine Water and the Environment 41 (1), 210-224
680
681 Oyarzun, R., Guevara, S., Oyarzún, J., Lillo, J., Maturana, H., Higueras, P. 2006. The As-contaminated Elqui
682 river basin: a long lasting perspective (1975-1995) covering the initiation and development of Au-Cu-As
683 mining in the high Andes of northern Chile. Environmental Geochemistry and Health 28, 431-443
684
685 Oyarzun, R., Lillo, J., Oyarzún, J., and Higueras, P. 2007. Plate interactions, evolving magmatic styles, and
686 inheritance of structural paths: development of the gold-rich, Miocene El Indio epithermal belt, northern
687 Chile. International Geology Review 49, 844-853
688
689 Romero, H., Rovira, A., Véliz, G. 1988. Geografía IV Región de Coquimbo. Colección de Geografía de
690 Chile, Instituto Geográfico Militar. Santiago, Chile.
691
692 Ruiz Pereira, S., Díez, B., Cifuentes-Anticevic, J., Leary, S., Fernandoy, F., Marquardt, C., Lambert, F. 2023.
693 Hydrological connections in a glaciated Andean cacthment under permafrost conditions (33º S). Journal of
694 Hydrology: Regional Studies 45, 101311. https://doi.org/10.1016/j.ejrh.2022.101311
695
696 Sarricolea, P., Herrera-Ossandon, M., Meseguer-Ruiz, O. 2017. Climatic regionalisation of continental Chile
697 Journal of Maps 13(2), 66-73. https://doi.org/10.1080/17445647.2016.1259592
698
699 Schaffer, N., MacDonell, S., Reveillet, M., Yañez, E., Valois, R. 2019. Rock glaciers as a water resource in
700 a changing climate in the semiarid Chilean Andes. Regional Environmental Change 19, 1263-1279
701
702 Sibson, R.H. 1987. Earthquake rupturing as a mineralizing agent in hydrothermal systems. Geology 15, 701-
703 704
704

Sibson, R.H., Moore, J.M., Rankin, A.H. 1975. Seismic pumping-a hydrothermal fluid transport mechanism. Journal of the Geological Society 131, 653-659

Sibson, R.H., Robert, F., Poulsen, K.H. 1988. High-angle reverse faults, fluid-pressure cycling, and mesothermal gold-quarts deposits. Geology 16 551-555

Sibson, R.H., 1990. Faulting and fluid flow. In: Fluids in Tectonically Active Regimes of the Continental Crust, Nesbitt, B.E. (Ed.), Short Course, Mineralogical Association of Canada, Vancouver, 93-132

Sommers, L.D., McKenzie, J.M. 2020. A review of groundwater in high mountain environments. WIREs WATER, 7:e1475. https://doi.org/10.1002/wat2.1475

Stewart, M.K., Morgenstern, U. 2016. Importance of tritium-based transit times in hydrological systems. WIREs Water 3, 145-154

Strauch, G., Oyarzun, J., Fiebig-Wittmaack, M., González, E., Weise, S.M. 2006 Contributions of the different water sources to the Elqui river runoff (northern Chile) evaluated by H/O isotopes. Isotopes in Environmental and Health Studies 42(3), 303-322. DOI 10.1080/10256010600839707

Taucare, M., Viguier, B., Daniele, L., Heuser, G., Arancibia, G., Leonardi, V. 2020. Connectivity of fractures and groundwater flows analyses into the Western Andean Front by means of a topological approach (Aconcagua Basin, Central Chile). Hydrogeology Journal 28, 2429–2438. https://doi.org/10.1007/s10040-020-02200-3

Tripp, G.I., Vearncombe, J.R. 2004. Fault/fracture density and mineralization: a contouring method for targeting in gold exploration. Journal of Structural Geology 26, 1087-1108

Valois, R., Araya, J., MacDonell, S., Guzmán, C., Fernandoy, F. Yáñez, G., Cuevas, J., Sproles, E., Maldonado, A. 2021. Improving the underground structural characterization and hydrological functioning of an Andean peatland using geoelectrics and water stable isotopes in semi-arid Chile. Environmental Earth Sciences 80, 41. https://doi.org/10.1007/s12665-020-09331-6

737 Vega-Briones, J., de Jong, S., Galleguillos, M., Wanders, N. 2023. Identifying driving processes of drought
738 recovery in the southern Andes natural catchments. Journal of Hydrology: Regional Studies, 47.
739 https://doi.org/10.1016/j.ejrh.2023.101369
740
741 Viviroli, D., Kummu, M., Meybeck, M., Kallio, M., Wada, Y. 2020. Increasing dependence of lowland
742 populations on mountain water resources. Nature Sustainability, *3*(11), 917-928.
743 https://doi.org/10.1038/s41893-020-0559-9
744
745 Vuille, M., Franquist, E., Garreaud, R., Lavado, W., Cáceres, B. 2015. Impact of the global warming hiatus
746 on Andean temperature. Journal of Geophysical Research: Atmosphere, 120, 3745–3757.
747 doi:10.1002/2015JD023126
748
749 Yáñez, E., Pascual, J.A., MacDonell, S. 2023. Hydrological response of a headwater catchment in the semi-
750 arid Andes (30ºS) to climate change. Journal of Water & Climate Change 14(10), 3617. DOI
751 10.2166/wcc.2023.268
752
753 Zhang, J., Guo, L., Mu, W., Liu, S., Zhao, D. 2021. Water-inrush risk through fault zones with multiple karst
754 aquifers underlying the coal floor: A case study in the Liuzhuang coal mine, Southern China. Mine Water
755 and the Environment 40, 1037-1047
756
757

Supplementary Material.

Raw Isotopic data

N°	Date	Sub-basin	$\delta^{18}O$	$\delta^{2}H$	^{3}H
			(‰)	(‰)	(TU)
1	2021-08-12	Derecho	-13.7	-99.3	1.292
2	2021-09-09	Derecho	-13.6	-98.7	
3	2021-10-20	Derecho	-13.3	-98.1	
4	2021-11-17	Derecho	-13.2	-97.8	
5	2021-12-15	Derecho	-13.3	-97.7	1.139
6	2022-01-17	Derecho	-13.1	-96.8	
7	2022-01-31	Derecho	-13.0	-96.9	
8	2022-03-15	Derecho	-13.3	-97.4	
9	2022-04-21	Derecho	-13.0	-97.4	
10	2022-05-24	Derecho	-13.5	-98.6	
11	2022-06-16	Derecho	-13.2	-99.3	
12	2022-07-12	Derecho	-13.6	-99.9	
13	2022-08-18	Derecho	-13.5	-99.9	1.329
14	2022-09-21	Derecho	-13.3	-99.2	
15	2022-10-20	Derecho	-13.2	-99.0	
16	2022-12-08	Derecho	-13.0	-96.8	1.519
17	2022-12-27	Derecho	-13.0	-95.4	
18	2023-01-24	Derecho	-13.2	-97.0	
19	2023-03-07	Derecho	-13.0	-97.0	
20	2023-04-13	Derecho	-13.1	-97.9	
21	2023-05-11	Derecho	-13.2	-98.8	
22	2023-06-21	Derecho	-13.4	-99.6	
23	2023-07-26	Derecho	-13.2	-98.8	
24	2023-08-31	Derecho	-13.2	-98.3	
25	2024-01-09	Derecho			1.102

763

N°	Date	Sub-basin	$\delta^{18}O$	$\delta^{2}H$	^{3}H
			(‰)	(‰)	(TU)
1	2021-08-12	Cochiguaz	-14.2	-103.3	1.357
2	2021-09-09	Cochiguaz	-14.0	-102.3	
3	2021-10-20	Cochiguaz	-13.6	-100.9	
4	2021-11-17	Cochiguaz	-13.5	-100.2	
5	2021-12-15	Cochiguaz	-13.5	-100.0	1.152
6	2022-01-17	Cochiguaz	-13.4	-99.0	
7	2022-01-31	Cochiguaz	-13.4	-99.5	
8	2022-03-15	Cochiguaz	-13.6	-100.0	
9	2022-04-21	Cochiguaz	-13.6	-100.7	
10	2022-05-24	Cochiguaz	-13.8	-101.8	
11	2022-06-16	Cochiguaz	-13.9	-102.8	
12	2022-07-12	Cochiguaz	-14.3	-104.8	
13	2022-08-18	Cochiguaz	-14.0	-103.5	1.479
14	2022-09-21	Cochiguaz	-13.8	-102.7	
15	2022-10-20	Cochiguaz	-14.0	-103.9	
16	2022-12-08	Cochiguaz	-13.6	-101.8	1.712
17	2022-12-27	Cochiguaz	-13.4	-101.4	
18	2023-01-24	Cochiguaz	-14.0	-102.1	
19	2023-03-07	Cochiguaz	-13.8	-101.8	
20	2023-04-13	Cochiguaz	-13.9	-102.7	
21	2023-05-11	Cochiguaz	-14.1	-103.9	
22	2023-06-21	Cochiguaz	-13.9	-104.3	
23	2023-07-26	Cochiguaz	-14.1	-104.0	
24	2023-08-31	Cochiguaz	-13.8	-102.7	
25	2024-01-09	Cochiguaz			1.167

764

765

766

767

N°	Date	Sub-basin	$\delta^{18}O$	$\delta^{2}H$	^{3}H
			(‰)	(‰)	(TU)
1	2021-08-12	Incaguaz	-14.8	-111.1	1.199
2	2021-09-09	Incaguaz	-14.7	-110.8	
3	2021-10-20	Incaguaz	-14.5	-109.9	
4	2021-11-17	Incaguaz	-14.3	-108.6	
5	2021-12-15	Incaguaz	-14.4	-109.0	1.099
6	2022-01-17	Incaguaz	-14.3	-107.7	
7	2022-01-31	Incaguaz	-14.3	-108.4	
8	2022-03-15	Incaguaz	-14.6	-109.1	
9	2022-04-21	Incaguaz	-14.6	-110.0	
10	2022-05-24	Incaguaz	-14.8	-111.6	
11	2022-06-16	Incaguaz	-15.1	-112.5	
12	2022-07-12	Incaguaz	-15.3	-112.9	
13	2022-08-18	Incaguaz	-15.1	-113.2	2.073
14	2022-09-21	Incaguaz	-14.9	-112.2	
15	2022-10-20	Incaguaz	-14.7	-111.9	
16	2022-12-08	Incaguaz	-15.1	-114.2	
17	2022-12-27	Incaguaz	-15.0	-112.4	
18	2023-01-24	Incaguaz	-14.4	-110.0	
19	2023-03-07	Incaguaz	-14.5	-109.6	
20	2023-04-13	Incaguaz	-14.6	-111.0	
21	2023-05-11	Incaguaz	-15.0	-112.4	
22	2023-06-21	Incaguaz	-15.1	-113.4	
23	2023-07-26	Incaguaz	-14.9	-112.2	
24	2023-08-31	Incaguaz	-14.9	-112.2	
25	2024-01-09	Incaguaz			1.076

768

769

770

N°	Date	Sub-basin	$\delta^{18}O$	$\delta^{2}H$	^{3}H
			(‰)	(‰)	(TU)
1	2021-08-12	Toro	-14.9	-115.0	0.316
2	2021-09-09	Toro	-14.9	-114.7	
3	2021-10-20	Toro	-14.6	-113.2	
4	2021-11-17	Toro	-14.6	-113.1	
5	2021-12-15	Toro	-14.8	-114.1	0.354
6	2022-01-17	Toro	-14.7	-112.6	
7	2022-01-31	Toro	-14.8	-113.3	
8	2022-03-15	Toro	-14.8	-114.2	
9	2022-04-21	Toro	-14.9	-114.3	
10	2022-05-24	Toro	-15.2	-115.6	
11	2022-06-16	Toro	-15.3	-116.2	
12	2022-07-12	Toro	-15.3	-116.2	
13	2022-08-18	Toro	-15.3	-117.5	0.446
14	2022-09-21	Toro	-15.1	-116.2	
15	2022-10-20	Toro	-14.9	-115.4	
16	2022-12-08	Toro	-14.8	-113.8	1.154
17	2022-12-27	Toro	-14.9	-113.8	
18	2023-01-24	Toro	-14.8	-113.8	
19	2023-03-07	Toro	-14.8	-113.7	
20	2023-04-13	Toro	-14.8	-114.7	
21	2023-05-11	Toro	-15.0	-115.9	
22	2023-06-21	Toro	-15.6	-117.1	
23	2023-07-26	Toro	-14.8	-115.8	
24	2023-08-31	Toro	-14.8	-114.9	
25	2024-01-09	Toro			0.327

771

772

773